

Scalar Cross-Relaxation Detected in the NOESY Spectra of Oxazolidines and Thiazolidines

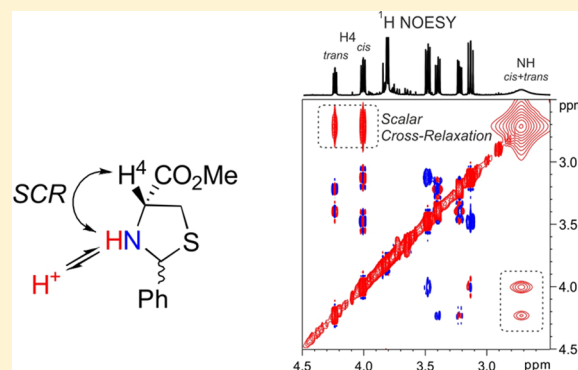
Tharindi D. Panduwawala,^{†,§} Laia Josa-Culleré,^{†,§} Ilya Kuprov,[‡] Barbara Odell,[†] Mark G. Moloney,^{*,†} and Timothy D. W. Claridge^{*,†}

[†]Department of Chemistry, Chemistry Research Laboratory, University of Oxford, Mansfield Road, Oxford OX1 3TA, U.K.

[‡]School of Chemistry, University of Southampton, Highfield Campus, Southampton SO17 1BJ, U.K.

S Supporting Information

ABSTRACT: Anomalous cross-peaks observed in the NOESY spectra of 2,4-disubstituted thiazolidines and oxazolidines that cannot be attributed to classical dipolar NOE or chemical exchange peaks have been investigated experimentally and computationally and have been shown to arise from scalar cross-relaxation of the first kind. This process is stimulated by the relatively slow modulation of scalar couplings and, for the systems studied, arises from slow on–off proton exchange of the amino nitrogen, a process influenced by solution temperature, acidity, and concentration. The mechanism is likely to be significant for many systems in which proton exchange occurs on the millisecond time scale, and misinterpretation of these cross-peaks may lead to erroneous conclusions should their true origins not be recognized.



INTRODUCTION

Nitrogen heterocycles comprise the core structural subunit in many alkaloids, and impart wide ranging biological and pharmaceutical activities.^{1,2} We have been interested in the elaboration of amino acid esters 1–3 to oxazolidines/thiazolidines *cis*-4 and *trans*-4 (where *cis* and *trans* defines the relative stereochemistry for the two positions adjacent to the ring nitrogen) and their use in turn as templates to direct aldol and Dieckmann ring annulation processes (Scheme 1).^{3–5} This chemistry may be applied to systems derived from serine 1,^{4,5} threonine 2,^{6,7} and cysteine 3,⁸ and the success of these processes critically depends on ring–chain tautomerism,^{9–12} which permits equilibration between *cis* and *trans* diastereomers 4, ultimately leading to the more stable product in which both substituents are pseudoequatorial, which is especially preferred when R' = *t*-Bu; this approach has shown synthetic value in the construction of antibacterial chemical libraries.¹³

During the synthesis of the oxazolidines and thiazolidines, prepared using literature protocols,^{4–8} mixtures of *cis* and *trans* diastereomers 4 were produced in ratios of ~1:1, which were difficult to separate by standard column chromatography. In the course of assigning the relative stereochemistry of these isomers, we were surprised to observe anomalous cross-peaks in 2D NOESY spectra that could not be explained by conventional analysis, as exemplified for 4d (Figure 1). This spectrum is unusual because in addition to the negative cross-peaks (colored blue) between CH protons indicative of the classical through-space nuclear Overhauser effect^{14,15} a number of strong positive cross-peaks (colored red) are also observed. Conventionally, for small molecules that do not aggregate, such peaks would be

suggestive of chemical exchange occurring between correlated protons,¹⁶ but here these are between protons that cannot possibly exchange with each other. Herein we rationalize the origin of these effects as arising from scalar cross-relaxation of the first kind (SCRKF), a process shown to be driven by NH proton exchange in these molecules. We believe it is likely that others will observe similar effects in NOE spectra in the presence of proton exchange and we present our investigations on the appearance of this effect in the title compounds to draw wider attention to this phenomenon.

RESULTS AND DISCUSSIONS

In a previous publication,¹⁷ anomalous NOESY cross-peaks similar to those in Figure 1 but observed for C-substituted aziridines could not be explained by dipolar cross-relaxation or chemical exchange and were shown, through experimental and computational studies, to arise from scalar relaxation of the first kind. The requirement for the associated scalar cross-relaxation process to occur, and be able to effectively compete with the dipolar cross-relaxation that is responsible for the classical NOE, is a modulation, on a millisecond time scale, of the coupling constant between *J*-coupled protons, such that the rate of longitudinal scalar cross-relaxation (expressed in eq 1) becomes significant:^{17,18}

Received: March 2, 2016

Published: May 5, 2016

Scheme 1. Thiazolidines (X = S) and Oxazolidines (X = O) Derived from Amino Acids and Aldehydes and the Corresponding Product Ratios in the Systems Studied by NMR

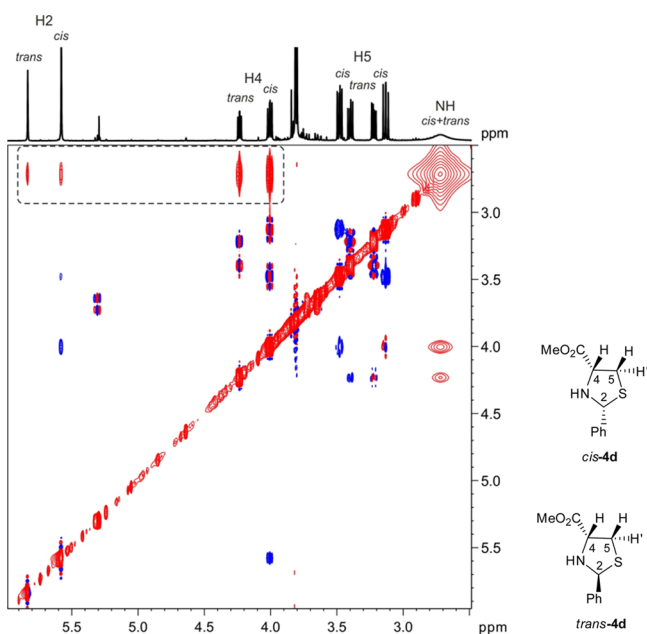
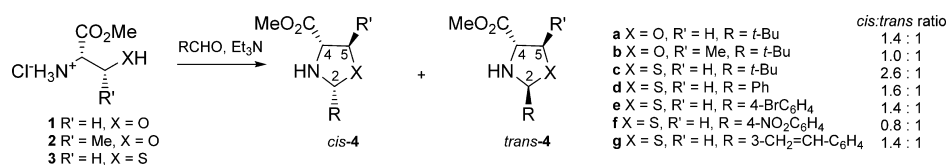


Figure 1. ¹H–¹H NOESY spectrum of **4d** as 1.6:1 *cis:trans* mixture (CDCl₃, 298 K, 500 MHz, 800 ms mixing time), showing anomalous strong positive cross-peaks (red) between the NH protons and those of the neighboring CH groups (boxed region).

$$\langle \hat{S}_Z^{(1)} | \hat{R}_{\text{SRFK}} | \hat{S}_Z^{(2)} \rangle = \frac{\Delta_J^2 \tau_{\text{ex}}}{2} \frac{1}{1 + (\omega_1 - \omega_2)^2 \tau_{\text{ex}}^2} \approx \frac{\Delta_J^2 \tau_{\text{ex}}}{2} \quad (1)$$

This expression shows that the cross-relaxation rate depends upon the size of modulation of scalar coupling constant (Δ_J), its rate of change (reflected in the lifetime of exchanging states τ_{ex}) and the frequency separation between the *J*-coupled protons ($\omega_1 - \omega_2$) in the ¹H spectrum. The effect is expected to be most pronounced for coupled protons with similar chemical shifts and where large modulations of coupling constants may occur. Notably, it gives rise to cross-peaks that have opposite sign to the NOEs typically observed for small molecules.

The NOESY spectrum of **4d** could be calculated theoretically using the Spinach simulation program^{19–21} to reproduce the anomalous cross peaks of **Figure 1** only when scalar cross-relaxation was included between the NH protons and their *J*-coupled neighbors H2 and H4 (**Figure 2**); without this term only classical dipolar NOEs were reproduced (see **Supporting Information** for details and **Figure S1**).

In the case of the aziridines,¹⁷ this scalar cross-relaxation process was shown theoretically to arise from the modulation of ¹H–¹H *J*-couplings of NH protons through conformational transitions involving nitrogen inversion. This is known to be relatively slow in aziridines due to the high inversion energy barriers involved (~ 70 kJ mol^{−1}), and hence gave rise to *J*-

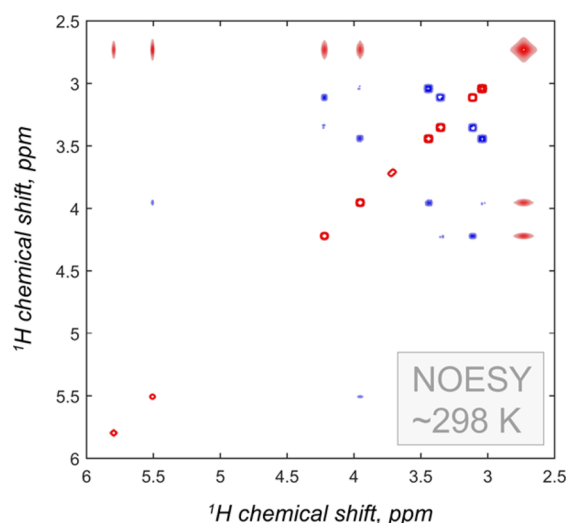


Figure 2. Simulated ¹H–¹H NOESY spectrum of **4d** (800 ms mixing time), exactly reproduces the positive cross-peaks of **Figure 1** only when scalar cross-relaxation of the first kind is considered between the amino protons and their *J*-coupled neighbors. Molecular geometries were obtained from DFT calculations, while chemical shifts and *J*-couplings of the individual *cis* and *trans* isomers were extracted from the experimental 1D NMR spectra. The proton exchange rate at the nitrogen center was set to 500 s^{−1}, overall rotational correlation time to 30 ps, nitrogen inversion correlation time to 100 μs, and modulation depth of *J*-coupling between the amino proton and the protons at C2 and C4 was set to 15 Hz (see main text for discussion of these parameters).

modulation rates appropriate for SCRFK to be operational and able to compete with the dipolar NOE.

We could find no reports on nitrogen inversion barriers in thiazolidines and oxazolidines in which the nitrogen is not fully substituted, although the free energy of activation for nitrogen inversion in *N*-methylthiazolidine is reported to be 35.9 kJ mol^{−1} (at the exchange coalescence temperature of 173 K).²² The inversion barrier in pyrrolidine is 25 kJ mol^{−1},²³ very much lower than in aziridines, and likely to be similar to those in oxazolidines and thiazolidines such as **4**. DFT calculations of the nitrogen inversion barrier do indeed suggest this to be the case (see **Supporting Information**), which places the nitrogen inversion time scale in the microsecond region at ambient temperatures. Such rates are too high to give rise to significant scalar cross-relaxation, and thus nitrogen inversion is not an appropriate mechanism to yield cross-peaks for the oxazolidine and thiazolidine systems which have NH proton scalar couplings of <15 Hz. Consistent with the absence of slow nitrogen inversion, only a single set of resonances was ever observed experimentally for each diastereoisomer of **4d** studied over a wide temperature range (193 to 298 K), and resonances from separate invertomers were never detected (in contrast to the aziridines where these were fully resolved in ¹H NMR spectra at 193 K¹⁷). This suggests that the process by which *J*-couplings are modulated to give rise

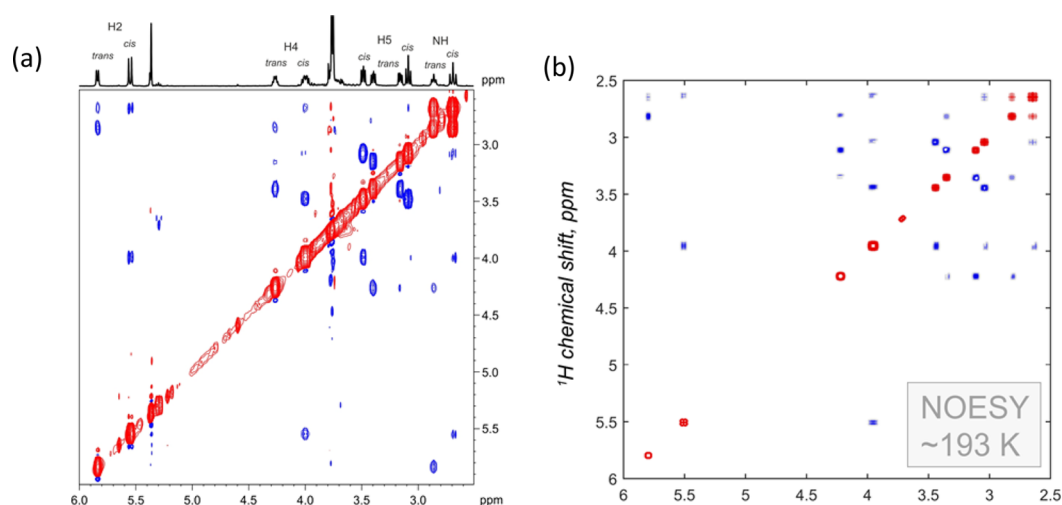
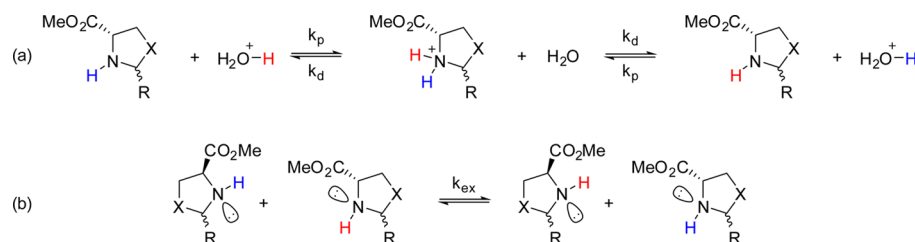


Figure 3. ^1H – ^1H NOESY spectrum (800 ms mixing time) of compound **4d**. (a) Mixture of *cis*/*trans* diastereoisomers in 1.6:1 ratio in CD_2Cl_2 at 193 K, showing only dipolar NOE (blue) and chemical exchange (red) cross-peaks. (b) A simulated NOESY spectrum ($\tau_c = 300$ ps), calculated using exchange rate constants of 0.25 and 0.5 s^{-1} (for *cis* and *trans* isomers, respectively) which reproduces all observed cross-peaks.

Scheme 2. Likely Proton Exchange Mechanisms in Thiazolidines ($\text{X} = \text{S}$) and Oxazolidines ($\text{X} = \text{O}$)^a



^a(a) acid catalysed proton exchange; (b) bimolecular proton exchange.

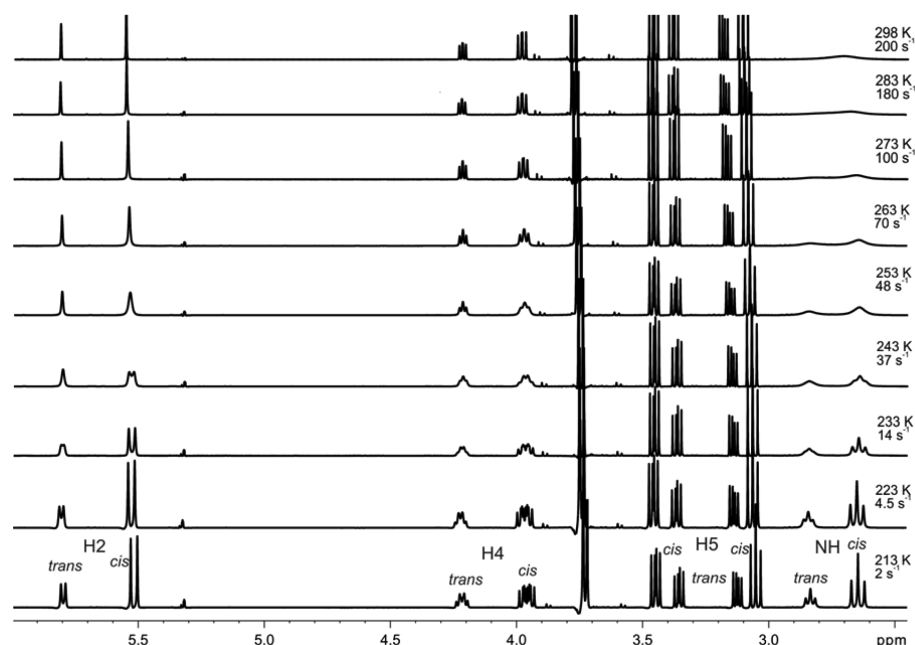


Figure 4. Variable temperature ^1H NMR spectra of **4d** in dried and degassed CD_2Cl_2 at 90 mM. The rate constants for two-site exchange between NH protons of the two diastereoisomers were determined by line shape fitting, with the lower rate constant listed.

to scalar cross-relaxation for **4d** must involve a different mechanism than direct nitrogen NH inversion.

Similar NOESY spectra exhibiting scalar cross-relaxation peaks between NH protons and adjacent CH protons were observed

for variously substituted thiazolidines and oxazolidines when studied at room temperature (see Figure S2). It was noticeable that the appearance of these cross-peaks was correlated with the presence of broad NH resonances without resolved *J*-coupling

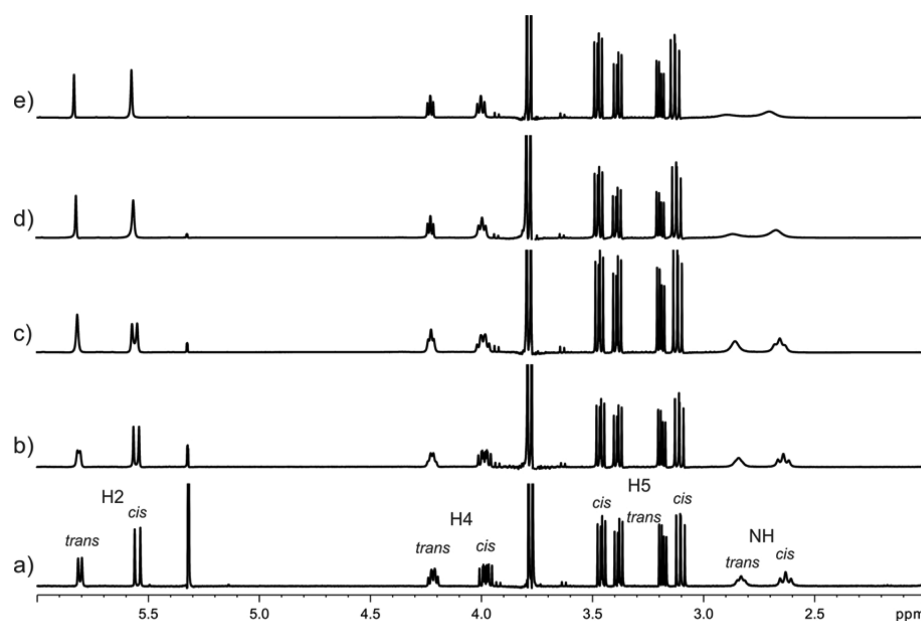


Figure 5. Concentration dependence of the NMR spectra of compound **4d** at 298 K in CD_2Cl_2 . (a) 8 mM; (b) 90 mM; (c) 270 mM; (d) 450 mM; (e) 900 mM.

structure for both *cis* and *trans* isomers; when the coupling fine structures of these resonances were well resolved, the anomalous cross-peaks were not seen. For example, the ^1H spectrum of **4d** recorded at 193 K showed clear NH coupling structure and the NOESY spectrum contained only intramolecular dipolar NOE peaks and chemical exchange peaks between the amino protons of the separate diastereoisomers, indicating these undergo slow intermolecular exchange (Figure 3). This suggests a likely process to cause modulation of J -couplings in the five-membered ring is a nitrogen protonation–deprotonation process, which could involve both acid-catalyzed and bimolecular pathways, in which water may also play a contributing role (Scheme 2). In the context of the SCRFK process, this would lead to variation of the scalar coupling since the incoming proton spin-state is uncorrelated with those of the remaining protons in the ring, a process also known to give rise to a loss of coupling structure, and often referred to as “exchange decoupling”. This process is clearly apparent in the variable temperature spectra of **4d** (Figure 4) where, as the NH resonances broaden, their coupling structure with the H2 and H4 resonances is progressively lost. Lineshape simulations of the spectra (Figure S3) provided estimates of the NH exchange rates between *cis/trans* diastereoisomers, which would likely be similar to those for exchange between similar stereoisomers (*cis/cis* or *trans/trans*) that would not normally be apparent in ^1H NMR spectra. These rates were used in simulations of NOESY spectra of **4d** to demonstrate the dependence on the scalar relaxation process on kinetic parameters (Figure S4), and these data clearly illustrate the progressive increase in SCRFK cross-peaks as the exchange rate increases and the NH J -coupling structure collapses. These data suggest that at rates below $\sim 50\text{ s}^{-1}$, SCRFK becomes inconsequential, while for rates at or above $\sim 200\text{ s}^{-1}$ (i.e., similar to those observed experimentally under ambient temperature conditions; Figure 4) this process is significant and gives rise to strong scalar cross-relaxation cross-peaks, as seen in Figure 1. In accord with this behavior, we have also observed that in situations when NH peaks display well-resolved multiplet structures and no SCRFK cross-peaks in NOESY

spectra, their appearance can be stimulated by raising the sample temperature to increase exchange rates such that NH coupling structure collapses. This may also be accompanied by evidence for NH exchange with residual water in the solvent (classical chemical exchange cross-peaks), as was observed for **4g** in toluene (Figure S5). It is also worth noting that for the chemical systems described here, the HN-H4 SCRFK cross-peaks always appear more intense than those for HN-H2 correlations, despite the similar J -coupling constants and the influence of identical exchange processes. This is a consequence of the smaller chemical shift separation in the case of HN-H4 and is consistent with the behavior anticipated from eq 1.

The proposed protonation–deprotonation cross-relaxation mechanism has been previously reported. Over 40 years ago, Fukumi et al. concluded that J -couplings were responsible for the sign change observed in the cross-relaxation rate between the OH and the CH protons in methanol²⁴ and ethanol²⁵ when acid concentration was varied. The corresponding theory originates from 1956,¹⁸ but, until recently,¹⁷ it appears that clear experimental manifestations of the process in molecules larger than HF, methanol, and ethanol are rare enough (or unusual enough) for the process to be commonly overlooked during NOESY data analysis. We believe this to be the first reported evidence for NH proton exchange yielding cross-peaks in NOESY spectra due to scalar cross-relaxation of the first kind.

Our investigations into these systems also demonstrated the appearance of these effects to be acutely sensitive to solution conditions, and specifically those that may influence NH exchange rates. For example, different batches of the CD_2Cl_2 solvent (prepared in different countries) gave different results: those that showed coalesced NH signals and SCRFK peaks in NOESY were suspected to contain traces of acid, whereas those that did not show these peaks were presumed to be less acidic. Consequently, the addition of trace amounts of deuterated acetic acid to the latter solutions of **4d** (0.01% v/v) was able to reintroduce these cross-peaks (Figure S6). The influence of traces of acid in sample workup procedures was also investigated in detail for **4d** where samples were dissolved in EtOAc and

washed with buffer at pH 5, 7, and 9 (see details in [Supporting Information](#)). Only the sample subjected to the pH 5 buffer gave rise to the SCRFK cross-peaks, while those from the higher pH buffers did not ([Figure S7](#)). Scalar cross-relaxation peaks were observed across a range of solvents including CD₂Cl₂, CDCl₃, C₆D₆, and toluene, although the exception was DMSO which appeared to inhibit these peaks, likely due to hydrogen-bonding perturbing the NH exchange process.

The likely involvement of bimolecular exchange was also seen to influence the proton spectrum of **4d** as a function of solution concentration ([Figure 5](#)). An increase was seen to lead to broadening of the NH resonance of both isomers with corresponding exchange decoupling of neighboring protons, indicative of an increase in exchange rate. Correspondingly, scalar cross-relaxation cross-peaks were observed only at the higher concentration for this sample. Slight shift changes are also apparent in the spectra of [Figure 5](#) as a function of concentration, most notably for the NH and the adjacent CH protons, which suggests association, potentially through intermolecular hydrogen bonding involving amino and carbonyl groups. Such association may promote the bimolecular exchange process and serve to enhance the appearance of scalar cross-relaxation. Thus, sample concentration will also likely dictate conditions under which scalar cross-relaxation peaks may be seen in NOESY spectra when proton exchange is involved, alongside temperature and solvent acidity.

CONCLUSIONS

The appearance of anomalous cross-peaks in the NOESY spectra of oxazolidines and thiazolidines has been attributed to scalar cross-relaxation of the first kind that arises when the *J*-couplings between correlated protons are slowly modulated. These cross-peaks have opposite sign to positive NOEs and an appearance similar to chemical exchange peaks, although they do not arise between mutually exchanging protons. For these systems, they are shown to arise from proton on–off exchange at the amino nitrogen which leads to modulation of proton scalar couplings, and their appearance is therefore sensitive to solution conditions that will influence this exchange rate, including sample temperature, solution acidity, and solute concentration. The presence of such peaks in (1D and 2D) NOESY spectra will likely occur in any system in which scalar couplings are modulated at an appropriate rate (on the millisecond time scale), with likely mechanisms including conformational interconversion, nitrogen inversion, and proton exchange.

EXPERIMENTAL SECTION

Synthesis. General Procedure for the Synthesis of Oxazolidine and Thiazolidine Compounds.²⁶ To the relevant methyl ester hydrochloride (1.0 equiv) in petroleum ether, triethylamine (1.5 equiv) and aldehyde (1.2 equiv) were added. The mixture was heated at reflux with continuous removal of water using a Dean–Stark head for 18 h. The white precipitate was then filtered and washed with Et₂O. The combined filtrates were concentrated under reduced pressure to give the oxazolidine or thiazolidine. All aryl substituted thiazolidines were purified by flash column chromatography (SiO₂, EtOAc/Petroleum ether).

Methyl (2*RS*,4*S*)-2-(*tert*-Butyl)-1,3-oxazolidine-4-carboxylate (4a**).**^{27,28} Yield (5.85 g, 97%); yellow oil; inseparable 1.4:1 *cis* and *trans* diastereomers. *R*_f (85% EtOAc in DCM) 0.64; ¹H NMR (400 MHz, CDCl₃) major isomer (*cis*): δ 4.07 (s, 1H, H₂), 3.89–3.97 (m, 2H, H_{5A} + H₄), 3.76 (s, 3H, CO₂CH₃), 3.68–3.72 (m, 1H, H_{5B}), 2.61 (br s, 1H, NH, averaged with *trans* isomer NH), 0.98 (s, 9H, C(CH₃)₃); minor isomer (*trans*): 4.32 (s, 1H, H₂), 4.11 (app t, 1H, *J* = 7.6 Hz, H_{5A}),

3.89–3.97 (m, 1H, H₄), 3.74 (s, 3H, CO₂CH₃), 3.68–3.72 (m, 1H, H_{5B}), 2.61 (br s, 1H, NH, averaged with *cis* isomer NH), 0.91 (s, 9H, C(CH₃)₃); ¹³C{¹H} NMR (100 MHz, CDCl₃) major isomer (*cis*): δ 173.0 (CO₂CH₃), 100.0 (C₂), 68.4 (C₄), 59.6 (C₅), 52.7 (CO₂CH₃), 33.3 (C(CH₃)₃), 25.3 (C(CH₃)₃); minor isomer (*trans*): 173.2 (CO₂CH₃), 99.3 (C₂), 69.0 (C₄), 59.5 (C₅), 52.5 (CO₂CH₃), 34.6 (C(CH₃)₃), 25.0 (C(CH₃)₃); IR (neat) $\nu_{\max}/\text{cm}^{-1}$ 3316, 2955, 1740; HRMS (TOF, ESI⁺) *m/z*: [M+H]⁺ Calcd for C₉H₁₈NO₃ 188.1281; Found 188.1285.

Methyl (2*RS*,4*S*,5*R*)-2-(*tert*-Butyl)-5-methyl-1,3-oxazolidine-4-carboxylate (4b**).** Yield (1.84 g, 77%); yellow oil; inseparable 1:1 diastereomers. *R*_f (50% EtOAc in DCM) 0.64; ¹H NMR (400 MHz, CDCl₃) (2*R*,4*S*,5*R*) isomer: δ 4.29 (s, 1H, H₂), 3.78–3.88 (m, 1H, H₅), 3.75 (s, 3H, CO₂CH₃), 3.46 (d, 1H, *J* = 7.2 Hz, H₄), 2.69 (br s, 1H, NH, averaged with 2*S*,4*S*,5*R* isomer NH), 1.33 (d, 3H, *J* = 6.0 Hz, C(S)CH₃), 0.97 (s, 9H, C(CH₃)₃); (2*S*,4*S*,5*R*) isomer: 4.38 (s, 1H, H₂), 3.78–3.88 (m, 1H, H₅), 3.77 (s, 3H, CO₂CH₃), 3.36 (d, 1H, *J* = 7.2 Hz, H₄), 2.69 (br s, 1H, NH, averaged with 2*R*,4*S*,5*R* isomer NH), 1.37 (d, 3H, *J* = 6.0 Hz, C(S)CH₃), 0.90 (s, 9H, C(CH₃)₃); ¹³C{¹H} NMR (100 MHz, CDCl₃) (2*R*,4*S*,5*R*) isomer: δ 172.1 (CO₂CH₃), 98.9 (C₂), 76.4 (C₅), 65.9 (C₄), 52.6 (CO₂CH₃), 34.7 (C(CH₃)₃), 24.9 (C(CH₃)₃), 20.0 (C(S)CH₃); (2*S*,4*S*,5*R*) isomer: 172.8 (CO₂CH₃), 98.3 (C₂), 77.4 (C₅), 67.2 (C₄), 52.5 (CO₂CH₃), 33.7 (C(CH₃)₃), 25.3 (C(CH₃)₃), 19.1 (C(S)CH₃); IR (neat) $\nu_{\max}/\text{cm}^{-1}$ 3315, 2957, 1741; HRMS (TOF, ESI⁺) *m/z*: [M+Na]⁺ Calcd for C₁₀H₁₉NNaO₃ 224.1257; Found 224.1266.

Methyl (2*RS*,4*S*)-2-(*tert*-Butyl)-1,3-thiazolidine-4-carboxylate (4c**).**²⁹ Yield (2.32 g, 98%); yellow oil; inseparable 2.6:1 *cis* and *trans* diastereomers. *R*_f (75% EtOAc in DCM) 0.61; ¹H NMR (500 MHz, CDCl₃) major isomer (*cis*): δ 4.43 (s, 1H, H₂), 3.78 (dd, 1H, *J* = 9.7, 6.7 Hz, H₄), 3.75 (s, 3H, CO₂CH₃), 3.23 (t, 1H, *J* = 10.2, 6.7 Hz, H_{5A}), 2.65 (t, 1H, *J* = 10.0 Hz, H_{5B}), 2.40 (br s, 1H, NH, averaged with *trans* isomer NH), 1.04 (s, 9H, C(CH₃)₃); minor isomer (*trans*): 4.50 (s, 1H, H₂), 4.11 (t, 1H, *J* = 6.0 Hz, H₄), 3.72 (s, 3H, CO₂CH₃), 3.08 (t, 1H, *J* = 10.6, 6.4 Hz, H_{5A}), 2.99 (dd, 1H, *J* = 10.6, 5.6 Hz, H_{5B}), 2.40 (br s, 1H, NH, averaged with *cis* isomer NH), 0.95 (s, 9H, C(CH₃)₃); ¹³C{¹H} NMR (100 MHz, CDCl₃) major isomer (*cis*): δ 171.9 (CO₂CH₃), 81.9 (C₂), 65.5 (C₄), 52.5 (CO₂CH₃), 37.5 (C₅), 34.1 (C(CH₃)₃), 27.1 (C(CH₃)₃); minor isomer (*trans*): 172.5 (CO₂CH₃), 79.9 (C₂), 65.1 (C₄), 52.5 (CO₂CH₃), 37.1 (C₅), 36.0 (C(CH₃)₃), 26.7 (C(CH₃)₃); IR (neat) $\nu_{\max}/\text{cm}^{-1}$ 3317, 2954, 1740; HRMS (TOF, ESI⁺) *m/z*: [M+Na]⁺ Calcd for C₉H₁₇NNaO₃ 226.0872; Found 226.0880.

Methyl (2*RS*,4*R*)-2-Phenyl-1,3-thiazolidine-4-carboxylate (4d**).** Yield (2.37 g, 91%); colorless oil; inseparable 1.6:1 *cis* and *trans* diastereomers; *R*_f (25% ethyl acetate in petroleum ether) 0.48; ¹H NMR (500 MHz, CDCl₃) major isomer (*cis*): δ 7.56–7.47 and 7.41–7.31 (m, 5H, Ar–CH), 5.57 (s, 1H, H₂), 3.99 (dd, 1H, *J* = 9.0, 7.0 Hz, H₄), 3.80 (s, 3H, CO₂CH₃), 3.47 (dd, 1H, *J* = 10.43, 7.0 Hz, H_{5A}), 3.12 (dd, 1H, *J* = 10.3, 9.0 Hz, H_{5B}), 2.70 (br. s, 1H, NH, averaged with *trans* isomer NH); minor isomer (*trans*): δ 7.41–7.31 (m, 5H, Ar–CH), 5.82 (s, 1H, H₂), 4.22 (dd, 1H, *J* = 7.1, 5.8 Hz, H₄), 3.79 (s, 3H, CO₂CH₃), 3.39 (dd, 1H, *J* = 10.6, 7.1 Hz, H_{5A}), 3.21 (dd, 1H, *J* = 10.6, 5.8 Hz, H_{5B}), 2.70 (br. s, 1H, NH, averaged with *cis* isomer NH); ¹³C{¹H} NMR (100 MHz, CDCl₃) major isomer (*cis*): δ 171.6 (CO₂CH₃), 138.2 (Ar–C), 128.7, 128.5, 127.5 (Ar–CH), 70.9 (C₂), 64.3 (C₄), 52.6 (CO₂CH₃), 39.2 (C₅); minor isomer (*trans*): δ 172.2 (CO₂CH₃), 141.2 (Ar–C), 128.7, 127.9, 127.0 (Ar–CH), 72.6 (C₂), 65.6 (C₄), 52.6 (CO₂CH₃), 38.2 (C₅); IR (neat) $\nu_{\max}/\text{cm}^{-1}$ 3314, 2952, 1736; HRMS (TOF, ESI⁺) *m/z*: [M+Na]⁺ Calcd for C₁₁H₁₃NNaO₃ 246.0559; Found 246.0563.

Methyl (2*RS*,4*R*)-2-(4-Bromophenyl)-1,3-thiazolidine-4-carboxylate (4e**).** Yield (5.60 g, 94%); colorless oil; inseparable 1.4:1 *cis* and *trans* diastereomers; *R*_f (20% ethyl acetate in petroleum ether) 0.23; ¹H NMR (500 MHz, C₆D₆) major isomer (*cis*): δ 7.39 (d, 2H, *J* = 8.5 Hz, Ar–CH), 7.30 (d, 2H, *J* = 8.4 Hz, Ar–CH), 5.40 (s, 1H, H₂), 3.87 (app t, 1H, *J* = 7.9 Hz, H₄), 3.70 (s, 3H, CO₂CH₃), 3.35 (dd, 1H, *J* = 10.4, 7.1 Hz, H_{5A}), 3.00 (dd, 1H, *J* = 10.3, 8.9 Hz, H_{5B}), 2.90–2.32 (br. s, 1H, NH, averaged with *trans* isomer NH); minor isomer (*trans*): δ 7.34 (d, 2H, *J* = 8.5 Hz, Ar–CH), 7.26 (d, 2H, *J* = 8.4 Hz, Ar–CH), 5.66 (s, 1H, H₂), 4.03 (app t, 1H, *J* = 6.5 Hz, H₄), 3.69 (s, 3H, CO₂CH₃), 3.27 (dd, 1H, *J* = 10.6, 7.1 Hz, H_{5A}), 3.06 (dd, 1H, *J* = 10.6, 6.1 Hz, H_{5B}), 2.90–

2.32 (br. s, 1H, NH, averaged with *cis* isomer NH); $^{13}\text{C}\{^1\text{H}\}$ NMR (100 MHz, CDCl_3) major isomer (*cis*): δ 171.4 (CO_2CH_3), 137.2, 122.5 (Ar-C), 131.7, 129.1 (Ar-CH), 71.0 (C2), 65.4 (C4), 52.6 (CO_2CH_3), 39.1 (C5); minor isomer (*trans*): δ 172.0 (CO_2CH_3), 140.5, 121.6 (Ar-C), 131.3, 128.6 (Ar-CH), 69.8 (C2), 64.0 (C4), 52.5 (CO_2CH_3), 38.0 (C5); IR (neat) $\nu_{\text{max}}/\text{cm}^{-1}$ 3313, 2951, 1737; HRMS (TOF, ESI^+) m/z : $[\text{M}+\text{H}]^+$ Calcd for $\text{C}_{11}\text{H}_{13}\text{O}_2\text{NBrS}$ 301.9845 and 303.9824; Found 301.9841 and 303.9818.

Methyl (2*RS*,4*R*)-2-(4-Nitrophenyl)-1,3-thiazolidine-4-carboxylate (4f).⁸ Yield (2.95 g, 94%); yellow oil; inseparable 0.8:1 *cis* and *trans* diastereomers; R_f (25% ethyl acetate in petroleum ether) 0.20; ^1H NMR (500 MHz, CDCl_3) major isomer (*trans*): δ 8.15 (d, 2H, $J = 8.8$ Hz, Ar-CH), 7.63 (d, 2H, $J = 8.5$ Hz, Ar-CH), 5.88 (s, 1H, H2), 4.08 (app t, 1H, $J = 6.6$ Hz, H4), 3.80 (s, 3H, CO_2CH_3), 3.39–3.35 (m, 1H, $\text{H}_{5\text{A}}$), 3.16–3.11 (m, 1H, $\text{H}_{5\text{B}}$), 2.65 (br. s, 1H, NH); minor isomer (*cis*): δ 8.20 (d, 2H, $J = 8.8$ Hz, Ar-CH), 7.69 (d, 2H, $J = 8.5$ Hz, Ar-CH), 5.60 (s, 1H, H2), 4.02 (app t, 1H, $J = 8.0$ Hz, H4), 3.81 (s, 3H, CO_2CH_3), 3.48 (dd, 1H, $J = 10.4$, 7.0 Hz, $\text{H}_{5\text{A}}$), 3.16–3.11 (m, 1H, $\text{H}_{5\text{B}}$), 3.05 (br. s, 1H, NH); $^{13}\text{C}\{^1\text{H}\}$ NMR (100 MHz, CDCl_3) major isomer (*trans*): δ 171.7 (CO_2CH_3), 149.5, 145.5 (Ar-C), 127.5, 123.5 (Ar-CH), 69.0 (C2), 64.1 (C4), 52.6 (CO_2CH_3), 38.1 (C5); minor isomer (*cis*): δ 171.2 (CO_2CH_3), 147.7, 147.1 (Ar-C), 128.4, 123.7 (Ar-CH), 70.9 (C2), 65.3 (C4), 52.6 (CO_2CH_3), 39.0 (C5); IR (neat) $\nu_{\text{max}}/\text{cm}^{-1}$ 3316, 1730, 1516, 1348; HRMS (TOF, ESI^+) m/z : $[\text{M}+\text{Na}]^+$ Calcd for $\text{C}_{11}\text{H}_{12}\text{N}_2\text{NaO}_4\text{S}$ 291.0410; Found 291.0405.

Methyl (2*RS*,4*R*)-2-(3-Vinylphenyl)-1,3-thiazolidine-4-carboxylate (4g). Yield (5.60 g, 84%); colorless oil; inseparable 1.4:1 *cis* and *trans* diastereomers; R_f (20% ethyl acetate in petroleum ether) 0.43; ^1H NMR (400 MHz, CDCl_3) major isomer (*cis*): δ 7.60–7.28 (m, 4H, Ar-CH), 6.79–6.69 (m, 1H, $\text{H}_{1'}$), 5.86–5.75 (m, 1H, $\text{H}_{2'_{\text{B}}}$), 5.58 (d, 1H, $J = 12.2$ Hz, H2), 5.33–5.26 (m, 1H, $\text{H}_{2'_{\text{A}}}$), 4.07–3.97 (m, 1H, H4), 3.83 (s, 3H, CO_2CH_3), 3.49 (dd, 1H, $J = 10.3$, 7.1 Hz, $\text{H}_{5\text{A}}$), 3.14 (dd, 1H, $J = 10.3$, 9.1 Hz, $\text{H}_{5\text{B}}$), 2.70 (app t, 1H, $J = 12.2$ Hz, NH); minor isomer (*trans*): δ 7.60–7.28 (m, 4H, Ar-CH), 6.79–6.69 (m, 1H, $\text{H}_{1'}$), 5.86–5.75 (m, 2H, $\text{H}_2 + \text{H}_{2'_{\text{B}}}$), 5.33–5.26 (1H, m, $\text{H}_{2'_{\text{A}}}$), 4.28–4.20 (m, 1H, H4), 3.82 (s, 3H, CO_2CH_3), 3.41 (dd, 1H, $J = 10.5$, 7.1 Hz, $\text{H}_{5\text{A}}$), 3.23 (dd, 1H, $J = 10.8$, 5.9 Hz, $\text{H}_{5\text{B}}$), 2.93–2.84 (1H, broad signal, NH); $^{13}\text{C}\{^1\text{H}\}$ NMR (100 MHz, CDCl_3) major isomer (*cis*): δ 171.5 (CO_2CH_3), 138.3, 138.0 (Ar-C), 136.3 (C1'), 128.8, 126.8, 126.4, 125.3 (Ar-CH), 114.5 (C2'), 72.4 (C2), 65.5 (C4), 52.5 (CO_2CH_3), 39.1 (C5); minor isomer (*trans*): δ 172.1 (CO_2CH_3), 141.4, 137.7 (Ar-C), 136.5 (C1'), 128.5, 126.3, 125.6, 124.8 (Ar-CH), 114.2 (C2'), 70.6 (C2), 64.2 (C4), 52.5 (CO_2CH_3), 38.0 (C5); IR (neat) $\nu_{\text{max}}/\text{cm}^{-1}$ 3305, 2951, 1737; HRMS (TOF, ESI^+) m/z : $[\text{M}+\text{H}]^+$ Calcd for $\text{C}_{13}\text{H}_{16}\text{O}_2\text{NS}$ 250.0896; Found 250.0890.

NMR Spectroscopy. NMR data were collected at 500 MHz (^1H) with sample temperatures over the range 193–373 K as stated. Samples were dissolved in dry C_6D_6 , CD_2Cl_2 , $\text{DMSO}-d_6$, or toluene- d_8 and characterized by ^1H , COSY, edited-HSQC, and ^{13}C NMR. 2D NOESY spectra were collected using standard pulse programs (90-t₁-90- τ_m -90-Acq, without or with a purging bipolar gradient pulse pair (+G₁[180]-G₁) at the midpoint of the mixing period, τ_m) with mixing times of 800 ms at the temperatures and in the solvents stated. For each data set, 8 or 16 transients were acquired for each of the 256 increments with 2K data points per spectrum, using a recovery time of 2 s. Data were processed typically as 1K × 1K data points using shifted squared-sinebell apodization windows. Typical sample concentrations for NOE analyses were in the range 8–450 mM. Probe temperature calibrations were performed using neat methanol samples containing a trace of HCl (below ambient) or with neat ethylene glycol (above ambient), and experiments were performed with active correction of the sample temperature set-points. Spectra were referenced to the residual ^1H solvent peak. ^1H NMR line shape simulations were performed using the gNMR³⁰ or SPINACH¹⁹ programs.

■ ASSOCIATED CONTENT

● Supporting Information

The Supporting Information is available free of charge on the ACS Publications website at DOI: 10.1021/acs.joc.6b00458.

Details of spectrum simulation methods, ^1H NOESY spectra, ^1H , and ^{13}C characterization spectra (PDF)

■ AUTHOR INFORMATION

Corresponding Authors

*mark.moloney@chem.ox.ac.uk

*tim.claridge@chem.ox.ac.uk

Author Contributions

[§]T.D.P. and L.J.-C. contributed equally to this work.

Notes

The authors declare no competing financial interest.

■ ACKNOWLEDGMENTS

L.J.C. received funding from the People Programme (Marie Curie Actions) of the European Union's Seventh Framework Programme (FP7/2007-2013) under REA grant agreement no. 316955. We also gratefully acknowledge funding under the MRC Confidence in Concept programme.

■ REFERENCES

- Royle, B. J. L. *Chem. Rev.* **1995**, *95*, 1981.
- Schober, R.; Schlenk, A. *Bioorg. Med. Chem.* **2008**, *16*, 4203.
- Jeong, Y.-C.; Anwar, M.; Nguyen, T. M.; Tan, B. S. W.; Chai, C. L. L.; Moloney, M. G. *Org. Biomol. Chem.* **2011**, *9*, 6663.
- Andrews, M.; Brewster, A.; Crapnell, K.; Ibbett, A.; Moloney, M. G.; Jones, T.; Prout, K.; Watkin, D. J. *Chem. Soc., Perkin Trans. 1* **1998**, 223.
- Andrews, M. D.; Brewster, A. G.; Moloney, M. G. *Synlett* **1996**, 1996, 612.
- Anwar, M.; Moloney, M. G. *Tetrahedron Lett.* **2007**, *48*, 7259.
- Heavyside, E. A.; Moloney, M. G.; Thompson, A. L. *RSC Adv.* **2014**, *4*, 16233.
- Anwar, M.; Moloney, M. G. *Chem. Biol. Drug Des.* **2013**, *81*, 645.
- Fulop, F.; Pihlaja, K.; Mattinen, J.; Bernath, G. *J. Org. Chem.* **1987**, *52*, 3821.
- Fulop, F.; Pihlaja, K.; Neuvonen, K.; Bernath, G.; Argay, G.; Kalman, A. J. *Org. Chem.* **1993**, *58*, 1967.
- Fülöp, F.; Pihlajaa, K. *Tetrahedron* **1993**, *49*, 6701.
- Lázár, L.; Göblyös, A.; Martinek, T. A.; Fülöp, F. *J. Org. Chem.* **2002**, *67*, 4734.
- Jeong, Y.-C.; Anwar, M.; Bikadi, Z.; Hazai, E.; Moloney, M. G. *Chem. Sci.* **2013**, *4*, 1008.
- Neuhaus, D.; Williamson, M. P. *The Nuclear Overhauser Effect in Structural and Conformational Analysis*, 2nd ed.; Wiley: New York, 2000.
- Claridge, T. D. W. *High-Resolution NMR Techniques in Organic Chemistry*, 2nd ed.; Elsevier: Oxford, 2009.
- Perrin, C. L.; Dwyer, T. J. *Chem. Rev.* **1990**, *90*, 935.
- Kuprov, I.; Hodgson, D. M.; Kloesges, J.; Pearson, C. I.; Odell, B.; Claridge, T. D. W. *Angew. Chem., Int. Ed.* **2015**, *54*, 3697.
- Solomon, I.; Bloembergen, N. *J. Chem. Phys.* **1956**, *25*, 261.
- Hogben, H. J.; Krzystyniak, M.; Charnock, G. T. P.; Hore, P. J.; Kuprov, I. *J. Magn. Reson.* **2011**, *208*, 179.
- Kuprov, I. *J. Magn. Reson.* **2011**, *209*, 31.
- Goodwin, D. L.; Kuprov, I. *J. Chem. Phys.* **2015**, *143*, 084113.
- Lehn, J.-M.; Wagner, J. *Tetrahedron* **1970**, *26*, 4227.
- Lehn, J.-M. *Fortsch. Chem. Forsch.* **1970**, *15*, 311.
- Fukumi, T.; Arata, Y.; Fujiwara, S. *J. Chem. Phys.* **1968**, *49*, 4198.
- Arata, Y.; Fukumi, T.; Fujiwara, S. *J. Chem. Phys.* **1969**, *51*, 859.
- Seebach, D.; Sting, A. R.; Hoffmann, M. *Angew. Chem., Int. Ed. Engl.* **1996**, *35*, 2708.
- Seebach, D.; Aebi, J. D. *Tetrahedron Lett.* **1984**, *25*, 2545.
- Seebach, D.; Aebi, J. D.; Gander-Coquoz, M.; Naef, R. *Helv. Chim. Acta* **1987**, *70*, 1194.
- Jeanguenat, A.; Seebach, D. *J. Chem. Soc., Perkin Trans. 1* **1991**, 2291.

(30) Budzelaar, P. H. M. *NMR simulation: gNMR*. <http://home.cc.umanitoba.ca/~budzelaar/gNMR/gNMR.html>.